

Energy band alignment at the nanoscale

Cite as: Appl. Phys. Lett. **110**, 051603 (2017); <https://doi.org/10.1063/1.4975644>

Submitted: 07 December 2016 • Accepted: 24 January 2017 • Published Online: 03 February 2017

 Jonas Deuermeier, Elvira Fortunato, Rodrigo Martins, et al.



View Online



Export Citation



CrossMark

ARTICLES YOU MAY BE INTERESTED IN

[Highly conductive grain boundaries in copper oxide thin films](#)

Journal of Applied Physics **119**, 235303 (2016); <https://doi.org/10.1063/1.4954002>

[Visualization of nanocrystalline CuO in the grain boundaries of Cu₂O thin films and effect on band bending and film resistivity](#)

APL Materials **6**, 096103 (2018); <https://doi.org/10.1063/1.5042046>

[Reactive magnetron sputtering of Cu₂O: Dependence on oxygen pressure and interface formation with indium tin oxide](#)

Journal of Applied Physics **109**, 113704 (2011); <https://doi.org/10.1063/1.3592981>



Webinar
Quantum Material Characterization
for Streamlined Qubit Development



Register now

Energy band alignment at the nanoscale

Jonas Deuermeier,^{1,2,a)} Elvira Fortunato,¹ Rodrigo Martins,¹ and Andreas Klein^{2,b)}

¹*3N/CENIMAT, Department of Materials Science, Faculty of Science and Technology, Universidade NOVA de Lisboa and CEMOP/UNINOVA, Campus de Caparica, 2829-516 Caparica, Portugal*

²*Department of Materials and Earth Sciences, Technische Universität Darmstadt, Jovanka-Bontschits-Straße 2, D-64287 Darmstadt, Germany*

(Received 7 December 2016; accepted 24 January 2017; published online 3 February 2017)

The energy band alignments at interfaces often determine the electrical functionality of a device. Along with the size reduction into the nanoscale, functional coatings become thinner than a nanometer. With the traditional analysis of the energy band alignment by *in situ* photoelectron spectroscopy, a critical film thickness is needed to determine the valence band offset. By making use of the Auger parameter, it becomes possible to determine the energy band alignment to coatings, which are only a few Ångström thin. This is demonstrated with experimental data of Cu₂O on different kinds of substrate materials. *Published by AIP Publishing.*

[<http://dx.doi.org/10.1063/1.4975644>]

The measurement of the energy band alignment between a film and a substrate material is possible by a step-wise procedure of alternating film deposition and *in situ* photoelectron spectroscopy. In the absence of chemical shifts and charging artifacts, the valence band offset is typically extracted at film thicknesses where a parallel shift of binding energies of the substrate and film emissions is observed.¹ The binding energy shift is a result of the charge exchange at the interface, since this creates charged states in the layers or at the interface. When the photoemission occurs in close proximity to the substrate (for example, in a very thin film), the substrate may affect the screening of the photoholes in the film material. This is mainly related to the influence of the substrate on the polarizability of electrons around the emission site in the film.² As a consequence, the binding energies of substrate and film emissions do not shift in parallel. In order to determine the valence band offset, a minimum film thickness is required, so that the substrate has no influence on the photoholes screening in the film.

The Auger parameter α' is sensitive to a change in polarizability, since the emission of a photoelectron creates a single excited state, whereas the Auger emission (AE) involves two ionized states.³ Therefore, tabulated values of α' are a widely used tool to obtain chemical state information from a material.⁴ Other than by a change in the oxidation state, a shift in α' can occur due to different coordinations of a metal cation (as it is the case of Al³⁺ in Al₂O₃, deposited on SiO₂).⁵ Furthermore, bridging oxygen between two different cations affects α' .⁶ The changes in the coordination number and bridging oxygen at an interface are rather short-ranged phenomena, since they depend on the bonding to the nearest neighboring ion/atom. An eventually different dielectric constant of the two materials forming the interface also affects the polarizability. The latter contribution extends further into the photoemitting material than the next neighboring environment.^{6,7}

An evaluation of the usefulness of the Auger parameter in order to correct the binding energies of film emissions for

the determination of the energy band alignment to the substrate is lacking. In this work, a set of experiments on different substrate materials is presented, in which the Auger parameter of copper oxide Cu₂O is used to remove the extra-atomic relaxation from the binding energy shifts towards the interface to the substrate. In this way, it is shown that such a correction of the measured binding energies reduces the critical film thickness for a determination of the valence band offset to a few Ångström.

Sample preparation for *in situ* X-ray photoelectron spectroscopy (XPS) was done at the DArmstadt Integrated SYstem for MATerial research (DAISY-MAT), a cluster tool which provides UHV transfer between deposition and characterization chambers.⁸ Cu₂O thin films were grown by reactive radio frequency (rf) magnetron sputtering without substrate heating. A 2 in. metallic copper target of 99.999% purity purchased from Lesker was sputtered at 25 W (2.53 W in.²) and 0.5 Pa total pressure. The stoichiometry of Cu₂O was optimized by adjusting the gas flow ratio of oxygen with respect to the total gas flow in the range of 3.7%–5.0%. The details on indicators for Cu₂O stoichiometry by *in situ* XPS can be found in the respective literature.^{9–11} The substrate materials which are analyzed in this work are Al₂O₃ by atomic layer deposition (ALD) as well as Bi₂O₃ and indium-tin oxide (ITO) by reactive rf magnetron sputtering. Al₂O₃ as substrate material was tested in two variants: First, a 250 nm thick multi-layer dielectric of alternating layers of Al₂O₃ and TiO₂ by ALD on ITO-coated glass was used, which is referred to as ATO and was provided by Planar Systems (now Beneq). The surface of this substrate consisted of 25 nm pure Al₂O₃. Second, 25 nm of Al₂O₃ was deposited on a commercial ITO-coated glass substrate in a custom-made ALD chamber. This substrate is referred to as *plain* Al₂O₃ in the remainder of this article. The parameters for a deposition at 200 °C are described elsewhere.¹² The deposition of 45 nm Bi₂O₃ by reactive rf magnetron sputtering was performed onto a commercial ITO-coated glass without intentional substrate heating according to the process described in a previous publication.¹¹ The ITO substrate was deposited on glass without intentional substrate heating according to the process described in previous work.¹⁰

^{a)}Electronic mail: j.deuermeier@campus.fct.unl.pt

^{b)}Electronic mail: aklein@surface.tu-darmstadt.de

XPS was performed in a Physical Electronics PHI 5700 multi-technique surface analysis unit, using monochromatic Al K α radiation with an energy of $h\nu = 1486.6$ eV, an emission angle of 45° , and a pass energy of 5.85 eV, resulting in an overall energy resolution of less than 0.4 eV.

The binding energy E_B is obtained by photoelectron spectroscopy as a positive value with respect to the Fermi energy E_F at $E_B = 0$. The magnitude of E_B is a function of the electron density at the emitting ion or atom.¹³ The binding energy would be purely determined by the *initial state* if the electron density remained “frozen” upon the creation of a photohole. In reality, the electron density around the emitting ion/atom screens the photohole due to relaxation processes, which constitute the *final state*.² The binding energy can be expressed as the difference between the initial state energy ϵ and the final state energy R .¹³ Shifts in binding energy of a photoelectron core level $\Delta E_B(\text{PE})$ with respect to an isolated state can have several reasons, which are generally categorized as initial state effects $\Delta\epsilon$ and final state effects ΔR .^{3,13,14}

It is useful for the here presented analysis to distinguish two effects separately, which contribute to a binding energy shift and are included in Eq. (1). Hollinger used ΔE_F to account for changes in Fermi energy at an interface between two materials.¹⁵ If thermodynamic equilibrium is assumed at a junction, it is of course the energy bands which change with respect to a constant Fermi energy. However, as the Fermi energy is used as reference energy in XPS, a parallel shift of energy bands may technically be expressed as a change in Fermi energy with the opposite sign. Iwata and Ishizaka, furthermore, added the term $e\Delta\Phi$ in order to account for the effects of charging, where e is the elementary charge.¹⁶ Charging due to photoemission of electrons always increases the binding energy, which is why its sign should be positive

$$\Delta E_B(\text{PE}) = \Delta\epsilon - \Delta R - \Delta E_F + e\Delta\Phi. \quad (1)$$

As mentioned earlier, only when the binding energy shift is exclusively due to the change in Fermi energy ΔE_F , the binding energies of substrate and film emissions shift in parallel and the valence band offset can be determined. This requires the knowledge of ΔR , besides a stable chemistry of the materials at the junction ($\Delta\epsilon = 0$) and the absence of charging artifacts ($e\Delta\Phi = 0$). In order to determine the change in relaxation energy ΔR , the Auger parameter α' can be used according to^{3,13}

$$\Delta R = \frac{\Delta\alpha'}{2}. \quad (2)$$

The relaxation phenomena, which determine ΔR , can be local (i.e., intra-atomic) or extra-atomic. Since Cu(I) does not undergo a local relaxation process,⁶ only extra-atomic relaxation is considered for the remainder of this article.

The Auger parameter is defined as the sum of the binding energy of the photoelectron $E_B(\text{PE})$ and the kinetic energy of the Auger electron $E_{\text{kin}}(\text{AE})$, which is equivalent to the difference between $E_B(\text{PE})$ and the binding energy at which the Auger emission appears in the spectrum $E_B(\text{AE}) = h\nu - E_{\text{kin}}(\text{AE})$ ¹³

$$\alpha' = E_B(\text{PE}) + E_{\text{kin}}(\text{AE}) = E_B(\text{PE}) + h\nu - E_B(\text{AE}). \quad (3)$$

With the changes in polarizability due to the proximity to an interface, a change in α' can be gradually observed towards low film thicknesses.^{17,18} Figure 1 shows a schematic example of how α' manifests in the binding energy shifts of Cu₂O close to the interface to a substrate material. Below a critical film thickness, ΔR is not equal to zero and can be calculated according to Equation (2). This allows to obtain the photoelectron binding energy shift due to the band bending $\Delta E_B^{\text{bb}}(\text{PE})$, which is free of extra-atomic relaxation caused by the vicinity of the substrate and is equivalent to a change in Fermi energy position due to the contact formation between the two materials

$$\Delta E_B^{\text{bb}}(\text{PE}) = \Delta E_B(\text{PE}) + \Delta R = -\Delta E_F. \quad (4)$$

The binding energy shifts of different core levels of the substrate and the film material were evaluated at each film thickness. Both for the substrate and film material, the shift is uniform for all core levels and can thus be represented by the respective valence band maximum. The results are displayed with respect to the film thickness in Figure 2. The core levels used for the calculation are indicated in the legend below the plots. The binding energy shift caused by the band bending $\Delta E_B^{\text{bb}}(\text{PE})$ is calculated using the Cu 2p emission and the Cu LMM Auger emission and represented in red. LMM refers to the orbitals in X-ray level notation, which are involved in the Auger emission, more precisely L₃M_{4,5}M_{4,5}. For each experiment, the valence band offset ΔE_{VB} is determined using both the non-corrected binding energy shifts (black vertical lines and numbers) and the binding energy shift of Cu 2p caused by the band bending (red vertical lines and numbers).

Figure 2(a) shows the results for the interface between Cu₂O and the ATO substrate. Charging effects due to the limited substrate conductance appear at intermediate thicknesses. However, the contribution $e\Delta\Phi$ is the same for both

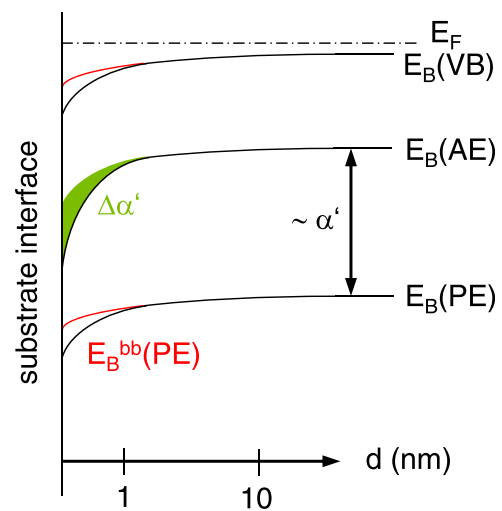


FIG. 1. Schematic representation of extra-atomic relaxation in Cu₂O at the interface to the substrate depending on the film thickness d . The measured binding energies E_B of the photoemission (PE) and the Auger emission (AE) as well as the valence band maximum (VB) are represented as black lines with respect to the Fermi energy E_F . The change in the Auger parameter $\Delta\alpha'$ is shown in green. When $\Delta R = \Delta\alpha'/2$ is added to the photoelectron binding energy, the red lines $\Delta E_B^{\text{bb}}(\text{PE})$ are obtained, which applies to all photoelectron emissions.

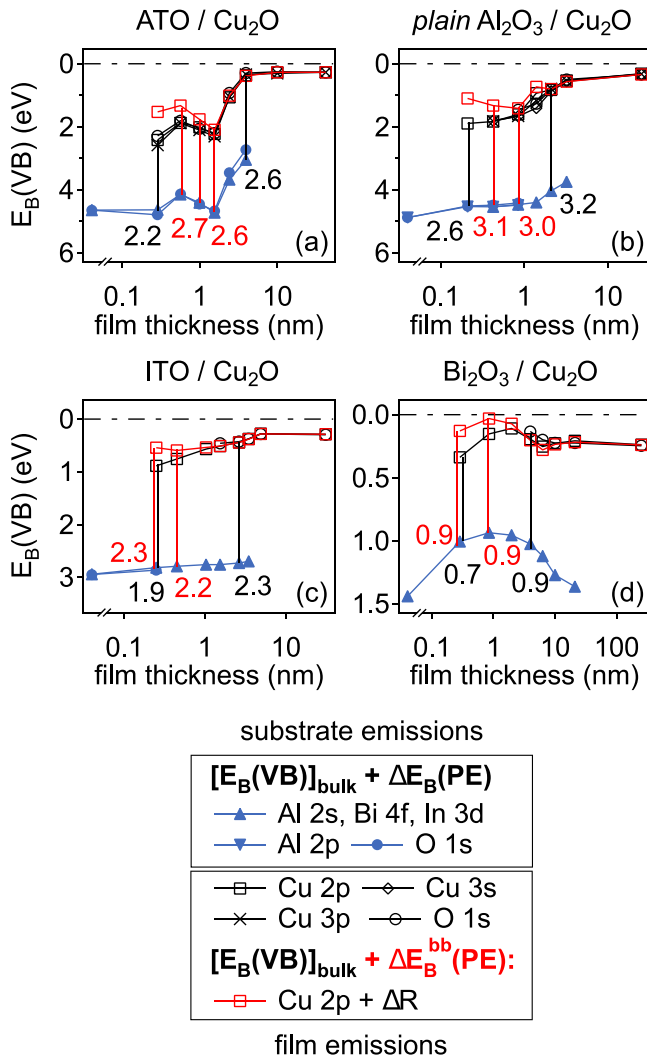


FIG. 2. The binding energy of the valence band maxima of Cu_2O films and of the different substrates are shown with respect to film thickness. In each representation, the binding energy increases from $E_F = 0$ eV towards the bottom. The evaluation of extra-atomic relaxation in Cu_2O is included as $\Delta E_B^{\text{bb}}(\text{PE})$ of the Cu 2p emission.

the substrate and the film emissions. Since artifacts due to charging were absent both in the measurement of the clean substrate and the film at final thickness, the evaluation of the valence band offset is not hindered. The respective value is found to range between 2.2 and 2.6 eV, when the measured Cu 2p binding energy is used for the calculation. Using $\Delta E_B^{\text{bb}}(\text{PE})$ leads to a constant value of $\Delta E_{\text{VB}} = 2.6$ eV between 0.6 and 4 nm film thickness.

The interface between *plain* Al_2O_3 and Cu_2O shown in Figure 2(b) reveals no sign of charging artifacts. This is probably due to a presumably better substrate conductance. Although all core levels of substrate and film individually show consistent shifts, there is some irregularity in the core level binding energies of the film material at 1.8 nm. The origin of this is not clear. ΔE_{VB} ranges from 2.6 to 3.2 eV when calculated from the measured binding energy shifts. The value corrected for the extra-atomic relaxation due to the substrate is 3.1 ± 0.1 eV between 0.4 and 4 nm film thickness.

The data presented in Figure 2(c) show Cu_2O on ITO. The core level binding energies are taken from previous work.¹⁰ In the original publication, the Auger parameter has

not been evaluated. Removing the additional extra-atomic relaxation caused by the substrate at a low film thickness allows us to determine a valence band offset of $\Delta E_{\text{VB}} = 2.2 - 2.3$ eV at film thicknesses between 0.3 and 3.5 nm.

Figure 2(d) shows the interface between Bi_2O_3 and Cu_2O . The consistency of the ΔE_{VB} quantification with respect to the film thickness can be improved, when the binding energy shift caused by the band bending $\Delta E_B^{\text{bb}}(\text{PE})$ is used. Then, a value of 0.9 eV is observed in a film thickness range between 0.3 and 6.3 nm.

A comparison of the different substrate materials in terms of their influence on ΔR with increasing thickness is given in Figure 3. It is observed that Al_2O_3 as substrate has a more severe effect on extra-atomic relaxation at low thicknesses of Cu_2O than Bi_2O_3 and ITO, the latter showing no significant difference between each other. Since the changes in polarizability due to different dielectric constants of the substrate ϵ_s and film materials ϵ_f are effective beyond the nearest neighbor environment, the corresponding polarization energy $U(d)$ shall be calculated here with respect to the film thickness d .^{7,17}

$$U(d) \approx \frac{\pi e^2}{8d} \left(\frac{1}{\epsilon_f} - \frac{1}{\epsilon_s} \right). \quad (5)$$

Bi_2O_3 has a dielectric constant of 40,¹⁹ compared to 9 of Al_2O_3 ,²⁰ which is rather similar to Cu_2O .²¹ Although ITO is not degenerately doped when deposited at room temperature, its dielectric constant is assumed to be infinite, similar to a metal. The resulting values are compared to ΔR in Figure 3.

Since $U(d)$ is positive whereas ΔR is negative, the different dielectric constants of substrate and film materials are not the main cause for the observed negative ΔR . However, since the effect is undoubtedly present, it may simply counteract a more prominent relaxation phenomenon at the interface. Such a compensation of a negative ΔR would be stronger for Cu_2O on ITO and Bi_2O_3 than for Cu_2O on Al_2O_3 . This interpretation is supported by a study in which Cu_2O was deposited on SiO_2 and ZrO_2 .²² SiO_2 has a lower dielectric constant than Cu_2O , whereas ZrO_2 a higher one.²⁰ $\Delta\alpha'$ towards low film coverages was found to be negative in both cases and to decrease more strongly on the less polarizable substrate (SiO_2) than on the one with higher polarizability (ZrO_2). This means that, for the results presented in this contribution, the change in polarizability by the substrate is predominantly related to the

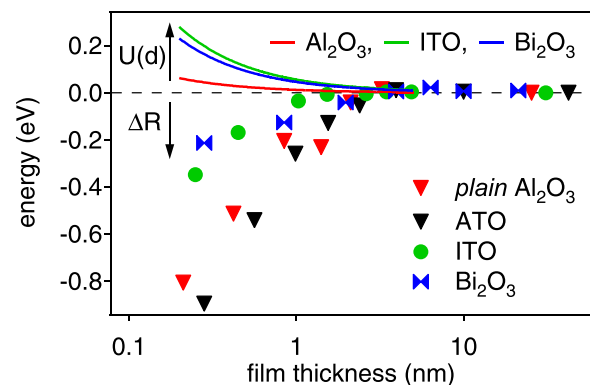


FIG. 3. Extra-atomic relaxation ΔR and polarization energy $U(d)$ with respect to Cu_2O thickness d on the different substrate materials.

chemical bonds between the substrate and film material and the resultant changes of cation coordination in the film.²³

In summary, it could be shown that it is possible to determine the energy band alignment by photoelectron spectroscopy between two materials, of which at least one is thinner than a nanometer. This was achieved by correcting the binding energy shift of the film emissions for the extra-atomic relaxation ΔR due to the vicinity of the substrate interface. The latter was quantified using the change in the Auger parameter. Since extra-atomic relaxation is an inherent effect of the photoemission process, it is concluded that the valence band offset between two materials is fully developed at a film thickness of a few Ångström. Using the described procedure, the valence band offsets between Cu_2O and Al_2O_3 by ALD (2.6 eV) as well as Cu_2O and Bi_2O_3 (0.9 eV) were determined.

This work was funded by FEDER funds through the COMPETE 2020 program and national funds through FCT—Portuguese Foundation for Science and Technology under the Project No. POCI-01-0145-FEDER-007688, Reference No. UID/CTM/50025 as well as SFRH/BD/77103/2011, UID/CTM/50025/2013, PEst-C/CTM/LA0025/2013-14 and EXCL/CTM-NAN/0201/2012. Furthermore, it has been supported by the German Science Foundation within the collaborative research center SFB 595 (Electrical Fatigue of Functional Material).

¹J. R. Waldrop, W. Grant, S. P. Kowalczyk, and E. A. Kraut, *J. Vac. Sci. Technol., A* **3**, 835 (1985).

²W. Egelhoff, *Surf. Sci. Rep.* **6**, 253 (1987).

³C. Wagner and A. Joshi, *J. Electron Spectrosc. Relat. Phenom.* **47**, 283 (1988).

⁴J. F. Moulder, W. F. Stickle, P. E. Sobol, and K. D. Bomben, *Handbook of X-ray Photoelectron Spectroscopy* (Physical Electronics, Inc., 1995).

⁵R. Reiche, F. Yubero, J. Espinós, and A. González-Elipe, *Surf. Sci.* **457**, 199 (2000).

⁶A. R. González-Elipe and F. Yubero, *Spectroscopic characterization of oxide/oxide interfaces, Handbook of Surfaces and Interfaces of Materials*, 2nd ed., edited by H. S. Nalwa (Academic Press, San Diego, 2001).

⁷J. G. Kirkwood, *J. Chem. Phys.* **2**, 351 (1934).

⁸A. Klein, *J. Am. Ceram. Soc.* **96**, 331 (2013).

⁹P. E. Larson, *J. Electron Spectrosc. Relat. Phenom.* **4**, 213 (1974).

¹⁰J. Deuermeier, J. Gassmann, J. Brötz, and A. Klein, *J. Appl. Phys.* **109**, 113704 (2011).

¹¹J. Deuermeier, H. F. Wardenga, J. Morasch, S. Siol, S. Nandy, T. Calmeiro, R. Martins, A. Klein, and E. Fortunato, *J. Appl. Phys.* **119**, 235303 (2016).

¹²T. J. M. Bayer, A. Wachau, A. Fuchs, J. Deuermeier, and A. Klein, *Chem. Mater.* **24**, 4503 (2012).

¹³C. D. Wagner, *Faraday Discuss. Chem. Soc.* **60**, 291 (1975).

¹⁴T. D. Thomas, *J. Electron Spectrosc. Relat. Phenom.* **20**, 117 (1980).

¹⁵G. Hollinger, *Appl. Surf. Sci.* **8**, 318 (1981).

¹⁶S. Iwata and A. Ishizaka, *J. Appl. Phys.* **79**, 6653 (1996).

¹⁷J. A. Mejías, V. M. Jiménez, G. Lassaletta, A. Fernández, and J. P. Espinós, *J. Phys. Chem.* **100**, 16255 (1996).

¹⁸R. Reiche, D. Dobler, J. P. Holgado, A. Barranco, A. I. Martín-Concepción, F. Yubero, J. P. Espinós, and A. R. González-Elipe, *Surf. Sci.* **537**, 228 (2003).

¹⁹J. Morasch, S. Li, J. Brötz, W. Jaegermann, and A. Klein, *Phys. Status Solidi A* **211**, 93 (2014).

²⁰J. Robertson, *Eur. Phys. J. Appl. Phys.* **28**, 265 (2004).

²¹P. Dawson, M. Hargreave, and G. Wilkinson, *J. Phys. Chem. Solids* **34**, 2201 (1973).

²²J. P. Espinós, J. Morales, A. Barranco, A. Caballero, J. P. Holgado, and A. R. González-Elipe, *J. Phys. Chem. B* **106**, 6921 (2002).

²³J. Morales, J. P. Espinós, A. Caballero, A. R. Gonzalez-Elipe, and J. A. Mejias, *J. Phys. Chem. B* **109**, 7758 (2005).

This article may be downloaded for personal use only. Any other use requires prior permission of the author and AIP Publishing. This article appeared in *Appl. Phys. Lett.* **110**, 051603 (2017) and may be found at <https://doi.org/10.1063/1.4975644>.

Available under only the rights of use according to UrhG.